Transactions, SMiRT-25
Charlotte, NC, USA, August 4-9, 2019
Division IV

FUNDAMENTAL STUDY ON WIND SHIELD STRUCTURES TO PROTECT EMERGENCY VEHICLES

Takahiro Murakami[1*], Hisato Matsumiya[2], Yuzuru Eguchi[1], Yoshiaki Nagata[3], Ichiro Tamura[3] and Tetsuya Hayashi[3]

[1] Senior Research Engineer*,Nuclear Risk Research Center, Central Research Institute of Electric Power Industry, Japan(murakami@criepi.denken.or.jp*)
[2] Civil Engineering Research Laboratory, Central Research Institute of Electric Power Industry, Japan
[3] Power Generation Div., The Chugoku Electric Power Co., Inc., Japan

ABSTRACT

An effective wind shield structure was studied to protect an emergence vehicle from tornado wind pressure. At first, a preliminary parametric survey was conducted using a computational method to identify important geometric parameters in designing a wind shield structure. Then, wind tunnel test was conducted to measure wind forces acting on a vehicle model with various spans of wind shield structures. Discuss was made to select a wind shield structure suitable to withstand the design wind speed.

INTRODUCTION

After the accident of the Fukushima Daiichi Nuclear Power Station, the New Regulatory Requirement demands to evaluate the impact of tornado on Nuclear Power Stations in Japan. The failure modes caused by tornado attack can be mainly classified into failures by wind pressure, failure by tornado-borne missile impact and flow path failure (blockage) by tornado-borne debris. In this study, we particularly place our focus on protective measures for emergency vehicles such as a water supply truck, which should withstand the tornado wind pressure, not only because it should be kept functional after tornado attack, but also because it should avoid to become tornado-borne missiles impacting on other safety-related facilities. A frequently-used method to prevent objects from moving is tie-down or anchoring of potential missiles by slings or bolts. However, anchoring emergency vehicles has an adverse effect for them, because they are required to be mobile as immediately as possible to act for an accident management plan. These situations have motivated us to study an effective configuration of wind shield structures (wind fence) to protect emergency vehicles without tie-down or anchoring, with ensuring the mobility.

In previous studies, aerodynamic features of high-sided vehicles were intensively investigated in the field of civil engineering. For example, Kopp et al. (2017) conducted wind-tunnel experiments under a straight wind condition using a scale-model of a box truck, and obtained wind speeds at overturning failure (e.g., 45-51m/s for fully loaded condition, 37-42 m/s for empty truck condition). Schmidlin et al. (2002) conducted wind-tunnel experiments under a straight wind condition using scale-models of sedan car and mini-ban to obtain upset wind speeds. They suggested that a stationary vehicle is unlike to be upset by winds less than about 50 m/s. Haan et al. (2017) conducted experiments under tornado-like vortex condition using scaled vehicle models of a mini-ban and a combine harvester to obtain wind speeds at sliding and lofting. The experimental results suggest that vehicle sliding can occur at EF1 wind speeds (40-50 m/s), while lofting at EF4 wind speeds (75-90 m/s). Bocciolone et al. (2008) measured aerodynamic forces acting on rail vehicles with wind tunnel experiments, showing significant effects of solid and porous wind fences on the aerodynamic forces. Alonso-Estebanez et al. (2017) computationally studied effect of a wind fence characteristics such as fence height, fence porosity, porosity configuration, and distance between fence and

a truck on cross-wind force acting on a truck on embankment road. Chen et al. (2015) experimentally studied aerodynamic effects of porous wind fence on vehicles running on bridges, while Xiang et al. (2018) similarly studied effect of a solid wind barrier on a vehicle on a bridge.

In this study, an effective wind shield structure similar to wind fence is computationally and experimentally searched in order to protect emergency vehicles from tornado wind in a nuclear power plant. Contrary to road and rail vehicles, such emergency vehicles are conservatively supposed to experience wind forces in every orientation with maximum wind speed of around 100 m/s. Then, we have to design a wind shield structure such that it can prevent emergency vehicles from failing under much more severe wind conditions than for road and rail vehicles. In the following, we present computational results obtained in a preliminary parametric survey to find out the important parameters of the geometric configuration in designing a wind shield structure. Next, we describe the experimental results obtained with a straight wind tunnel facility where we measured wind forces acting on a truck model. We discuss the effect of wind shield structure configuration on the wind forces, and present the conclusion in the final section.

PRELIMINARY SCREENING USING COMPUTATIONAL FLOW ANALYSIS

Computational Conditions

Figure 1 shows our basic design of wind shield structures with triangle cross-sections, and location of a high-sided vehicle represented by a rectangle. Two-dimensional wind flow computation has been conducted using the OpenFOAM 2.4.0 code for a preliminary parametric survey to screen out less significant parameters. Turbulent model employed is an RNG k-ε model, while inflow boundary condition is set by either uniform velocity profile or boundary layer velocity profile. Steady state solutions were obtained for the following cases. First, we computed flow around a real-scale vehicle model at a wind speed of 100 m/s without wind shield structures to evaluate the drag and lift forces. Next, we examined the influence of height and bottom width of triangular shields (H_{wall}, W_{all}) in order to select an effective shape of shield structures for a vehicle. Some computations were also conducted to see the effects of the height, H, bottom clearance, h and width, W of a vehicle. Furthermore, we evaluated the influence of the span of wind shied structures L (=$2d$+W) in order to consider multiple vehicles between a pair of wind shield structures.

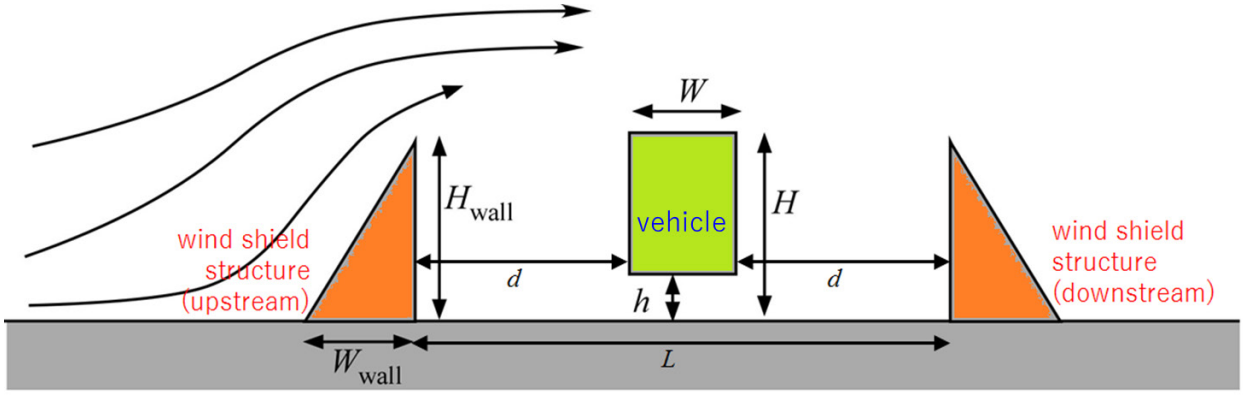

Figure 1. Geometry used for Two-dimensional wind flow computation.

Computational Results

Using the computational results, drag force and lift force acting on the vehicle model are computed by integrating pressure on the vehicle surface. Then, the results are analyzed in terms of drag coefficient, C_D, and lift coefficient, C_L, defined below.

$$C_D = \frac{F_D}{\frac{1}{2}\rho U^2(H-h)} = \frac{\int_S p(\mathbf{n}_D \cdot \mathbf{n}_S)dS}{\frac{1}{2}\rho U^2(H-h)} \quad (1)$$

$$C_L = \frac{F_L}{\frac{1}{2}\rho U^2 W} = \frac{\int_S p(\mathbf{n}_L \cdot \mathbf{n}_S)dS}{\frac{1}{2}\rho U^2 W} \quad (2)$$

Where F_D and F_L are respectively drag force and lift force acting on unit length of the vehicle model (rectangle), p and $\mathbf{n}_s$ are respectively the pressure and unit inward normal vector on the vehicle surface, S, while $\mathbf{n}_D$ and $\mathbf{n}_L$ are a unit vector orienting main flow direction and upward direction, respectively. Besides, ρ denotes air density, and U denotes main flow speed (100 m/s).

Figures 2 (a) and (b) respectively show drag and lift coefficients in variation with L, where vehicle height, H, bottom clearance, h, and width, W, are set at 3.5m, 0.4m, and 2.5m, respectively and the height of the wind shield structure, H_{wall}, is the same as the vehicle height. Both the figures show the drag and lift forces are reduced if span, L, is less than about 23.5m, while negative drag force (reversing force) and negative lift force (down force) become pronounced for the large span cases beyond 23.5m. The negative drag force can be explained by the flow pattern shown in Fig.3 for the case of 23.5m span. This figure shows large-scale recirculation (separation) region extending to the downstream of a pair of the wind shield structures, generating reversal flow around the vehicle. Figure 4 shows pressure distribution for the case corresponding to Fig.3. Significantly negative pressure between the lee side of the upstream wind shield structure and the vehicle can drive air beneath the separated main flow to move in a reverse direction.

All the computed results including the other cases not shown here indicate the followings.

(1) Geometry of the triangular shield structure such as ratio of H_{wall} against W_{all} does not have a significant impact on the drag force and lift force acting on the vehicle model.
(2) The height of the wind shield structure, H_{wall}, relative to the vehicle height, H, has a significant impact on the aerodynamic forces acting on the vehicle model.
(3) When the height of the wind shield structure, H_{wall}, is equal to the vehicle height, H, the shorter the span distance, L, is, the smaller the absolute values of the drag force and lift force acting on the vehicle model are.

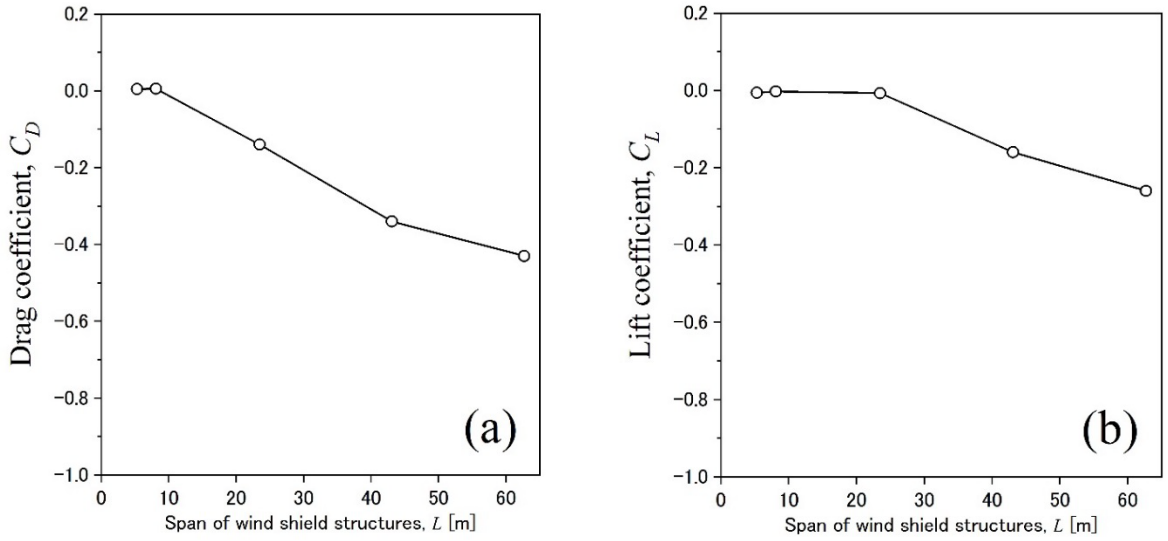

Figure 2. (a) Drag coefficient and (b) lift coefficient in variation with L.

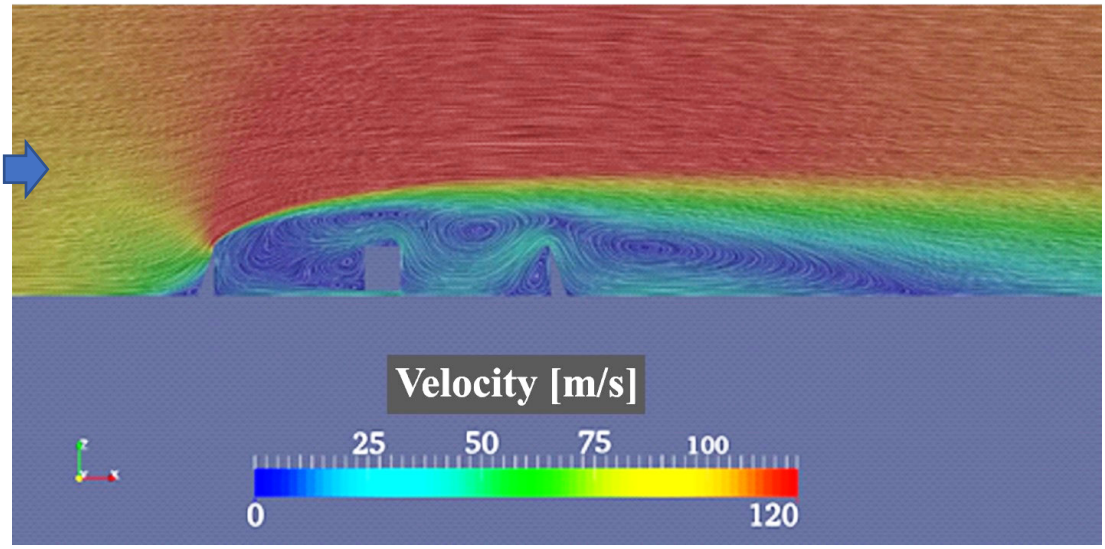

Figure 3. Wind speed and streamlines for 23.5m of span distance, *L*.

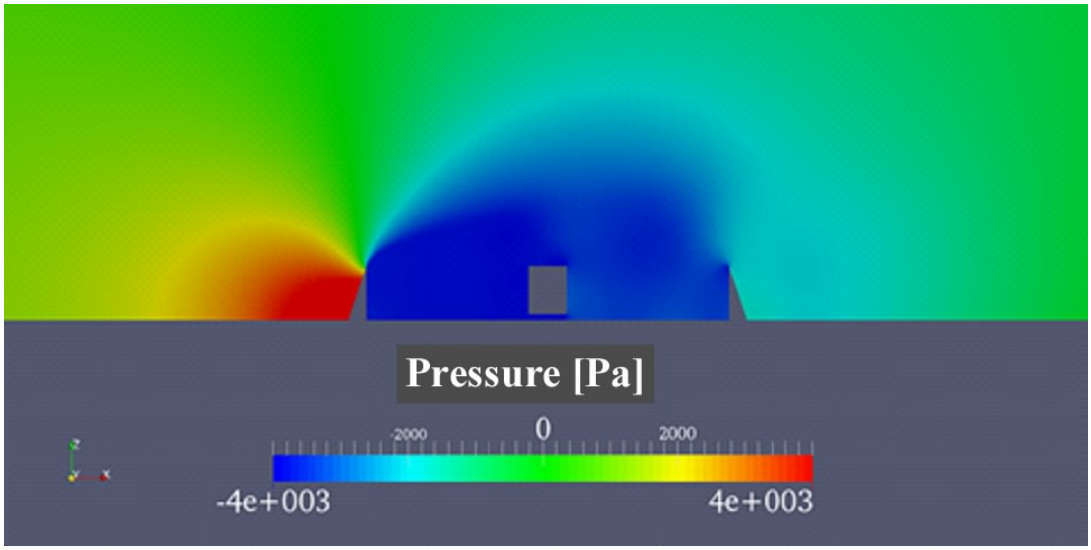

Figure 4. Pressure distribution for 23.5m of span distance, *L*.

WIND TUNNEL EXPERIMENTS

Experimental Conditions

Based on the 2-D analysis results, wind tunnel experiments were carried out using 3-demensional 1/50-scaled models of actual wind shield structures (Fig.5). The wind tunnel facility of CRIEPI (Central Research Institute of Electric Power Industry) is used for the experiments with average wind speed of 10 or 15 m/s. In this experiment, wind shield structures were placed on a turntable to change wind direction. A scaled vehicle model connected with a load cell (6-component dynamometer) is set at the center of the turntable for every case. The aerodynamic forces acting on a vehicle model were measured in the vehicle's reference system as shown in Fig.6.

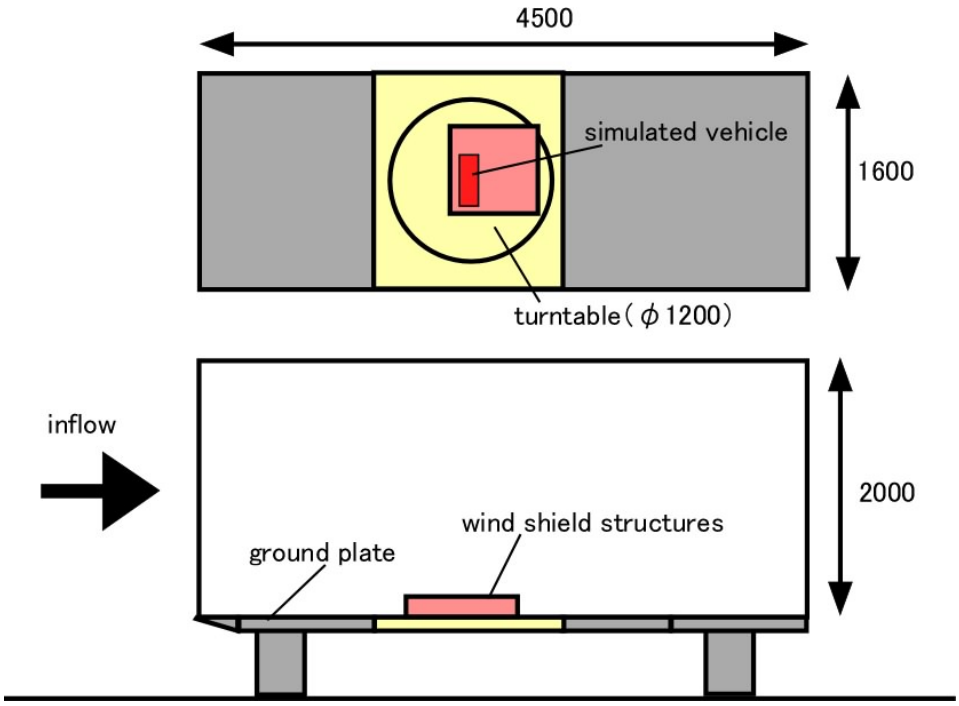

Figure 5. Setup of a scaled model in wind tunnel (upper: plan view, above: vertical view).

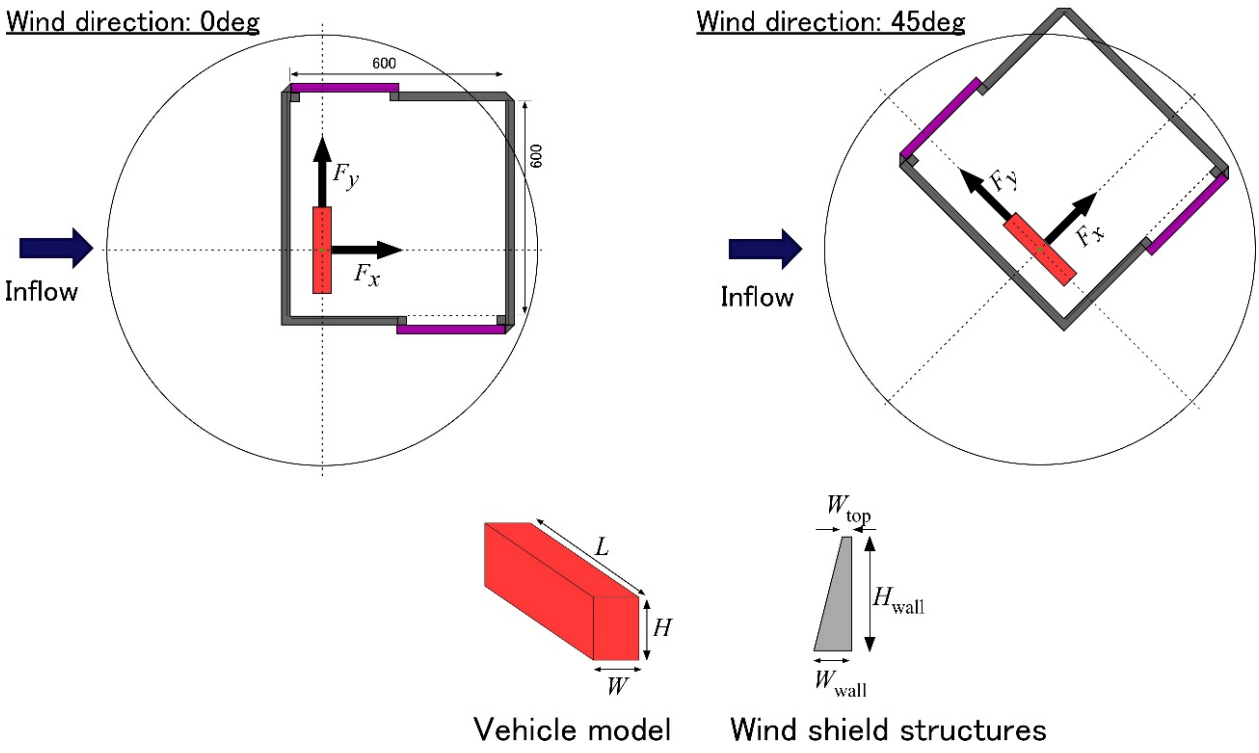

Figure 6. Wind direction and vehicle's reference system for aerodynamic force measurement.

Table 1 describes the dimensions of the 1/50 scale model used for the wind tunnel test, while Table 2 describes the experimental cases reported in this paper. Photos of scale models of a vehicle and wind shield structure (wall) used in the experimental cases are shown in Photos 1 (a) to (f).

Experimental Results

Since the side force, F_x, in vehicle's reference system and lift force, F_L, are the most important parameters, the side force coefficient, C_x, and lift force coefficient, C_L, defined below were evaluated for each case in variation with the wind direction.

$$C_x = \frac{F_x}{\frac{1}{2}\rho U^2 HL} \tag{3}$$

$$C_L = \frac{F_L}{\frac{1}{2}\rho U^2 WL} \tag{4}$$

Where H, W and L are height, width and length of the vehicle model, respectively, while ρ denotes air density, and U denotes average wind tunnel speed.

Figure 7 shows side force coefficient and lift force coefficient for Case2a (30m×30m, Center) and Case2b (30m×30m, near wall) with reference to Case 1. Figure 8 also shows the same coefficients for Case3a (20m×20m, Center) and Case3b (20m×20m, near wall) with Case 1, while Figure 9 for Case4 (30m×15m, near wall) and Case5 (20m×10m, Center). Figure 7 indicates that the side force acting on the vehicle protected by the 30m-by-30m structure considerably decreases in comparison with that of an unprotected vehicle. The lift force acting on the vehicle protected by the 30m-by-30m structure is almost always negative, while that of an unprotected vehicle varies in both negative and positive ranges, depending on the wind direction. The side force drastically decreases in the case of the 20m-by-20m shield structure as shown in Figure 8, and the lift force is almost always negative, meaning the vehicle is forced downward. The side force and lift force for Case 5 are considerably reduced, indicating wind speed is weak around the vehicle for any wind direction due to short distance between the vehicle and the wall. Figure 10 summarizes the maximum absolute value of side force coefficient of each experimental case at the most unfavourable wind direction for each case. This figure indicates that the side force acting on the vehicle protected by the 30m-by-30m structure decreases by about 50% in comparison with that of an unprotected vehicle, while the side force decreases by as much as 75% in the case of 20m-by-20m. The side force in Case 5 is the least among the cases reported here.

Table 1: Dimensions for a 1/50-scale model.

notation	Real scale	1/50-scale
L	12.0m	2.4cm
W	2.5m	5.0cm
H	3.3m	6.6cm
h	0.3m	0.6cm
H_{wall}	3.5m	7.0cm
W_{wall}	1.2m	2.4cm
W_{top}	0.2m	0.4cm

Table 2: Experimental cases

Case No.	Areas of wind shield structure	Position of the vehicle
1	No wind shield	-
2a	30m × 30m	Center
2b	30m × 30m	Near wall
3a	20m × 20m	Center
3b	20m × 20m	Near wall
4	30m × 15m	Near wall
5	20m × 20m	Center

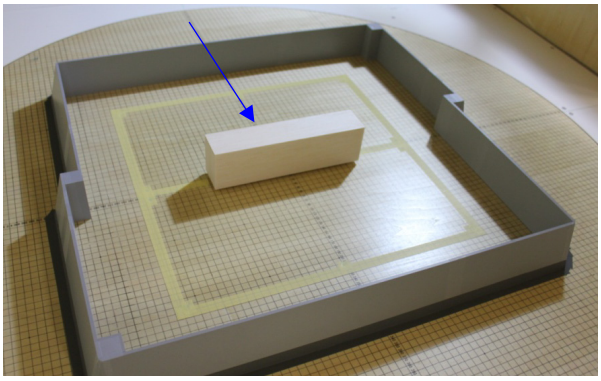

(a) Case2a (30m×30m, Center)

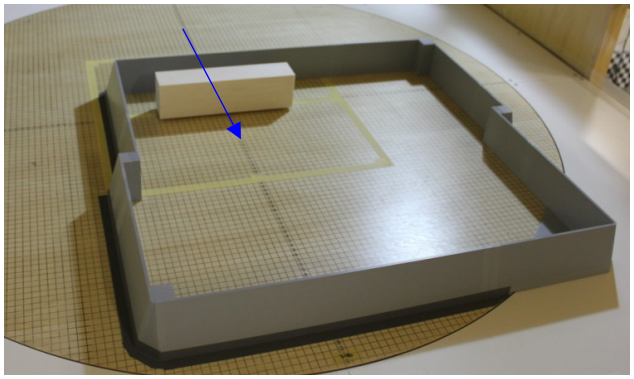

(b) Case2b (30m×30m, near wall)

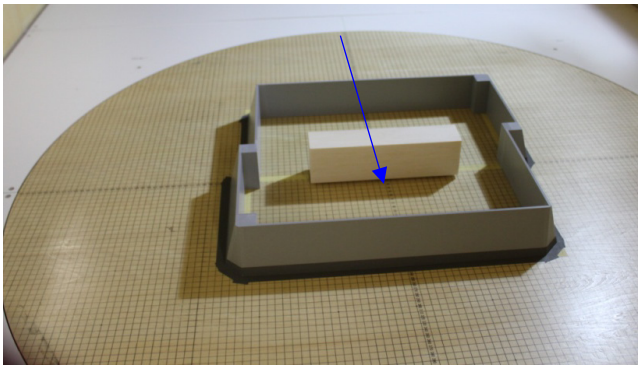

(c) Case3a (20m×20m, Center)

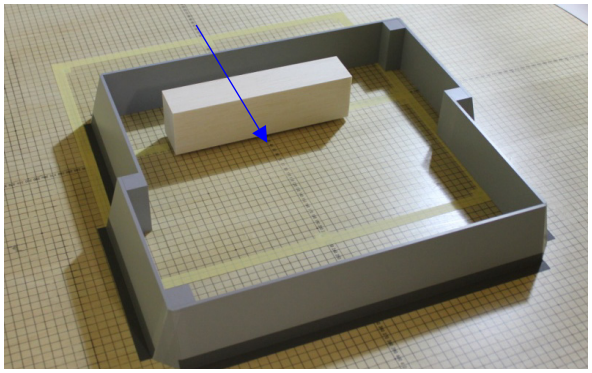

(d) Case3b (20m×20m, near wall)

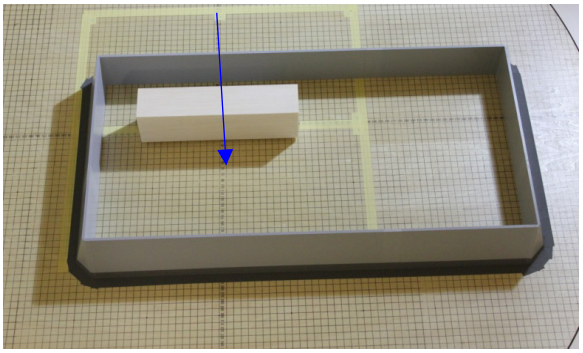

(e) Case4 (30m×15m, near wall)

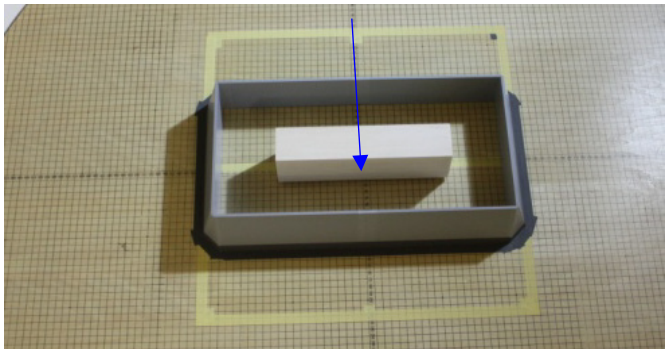

(f) Case5 (20m×10m, Center)

Photo 1. Scale model of a vehicle and a wind shield structure (arrows: 0-degree wind direction).

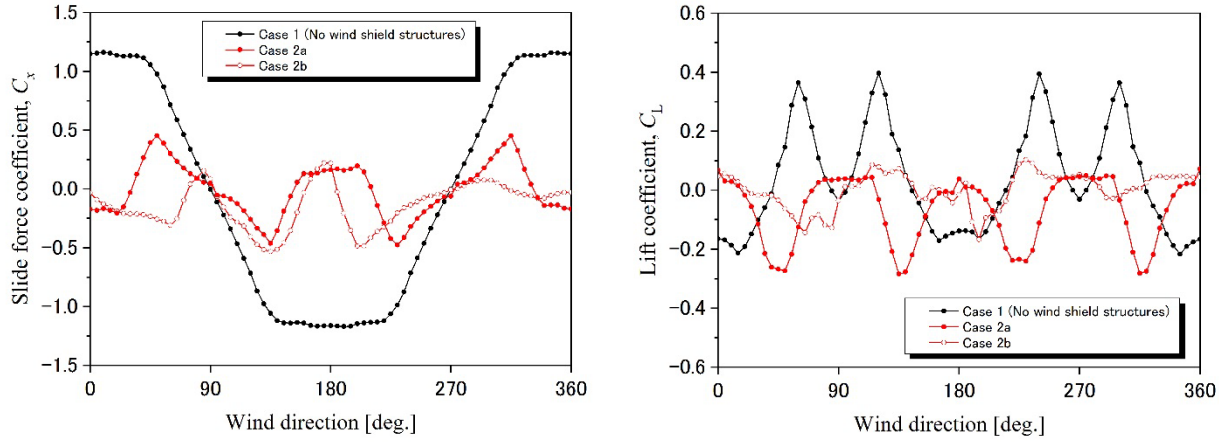

Figure 7. Side force coefficient (a) and lift force coefficient (b) for Case2a (30m×30m, Center) and Case2b (30m×30m, near wall) in reference to Case 1.

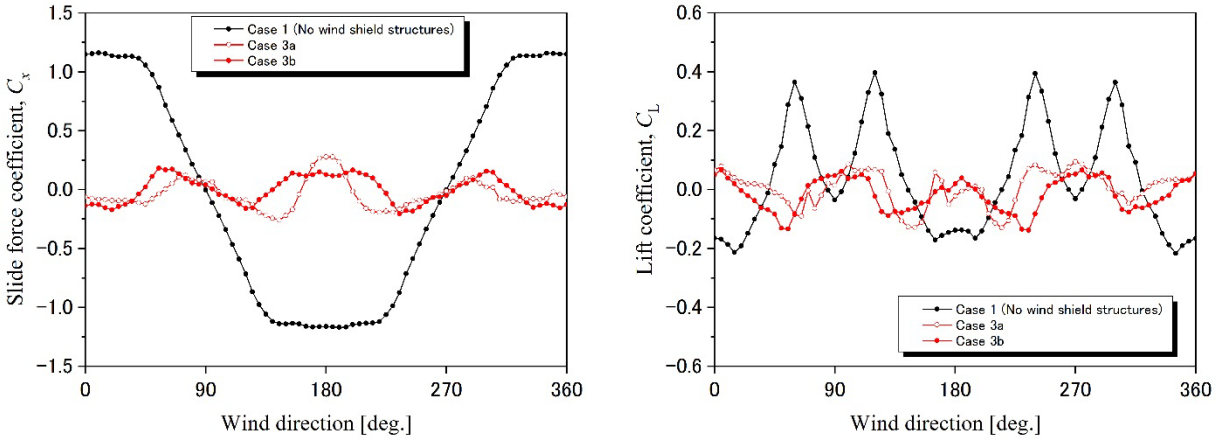

Figure 8. Side force coefficient (a) and lift force coefficient (b) for Case3a (20m×20m, Center) and Case3b (20m×20m, near wall)in reference to Case 1.

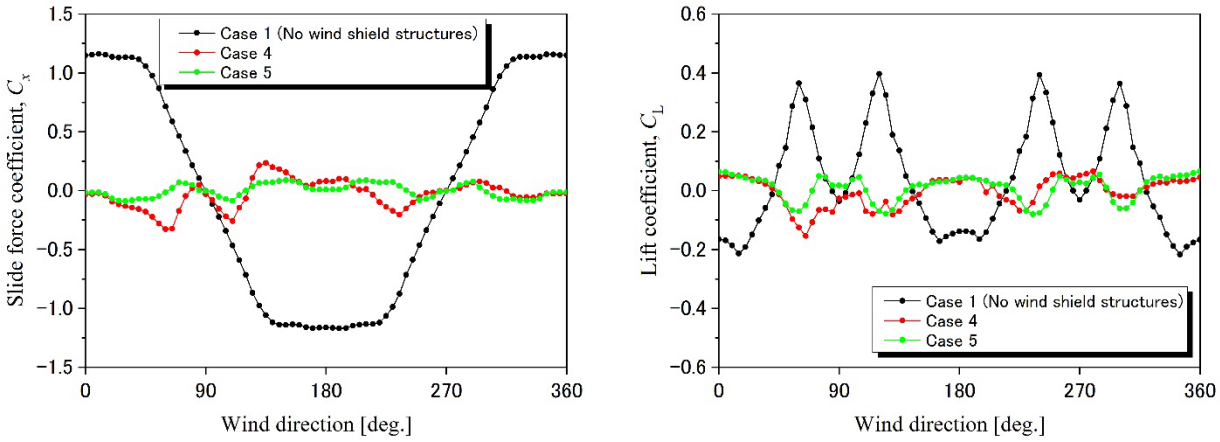

Figure 9. Side force coefficient (a) and lift force coefficient (b) for Case4 (30m×15m, near wall) and Case5 (20m×10m, Center) in reference to Case 1.

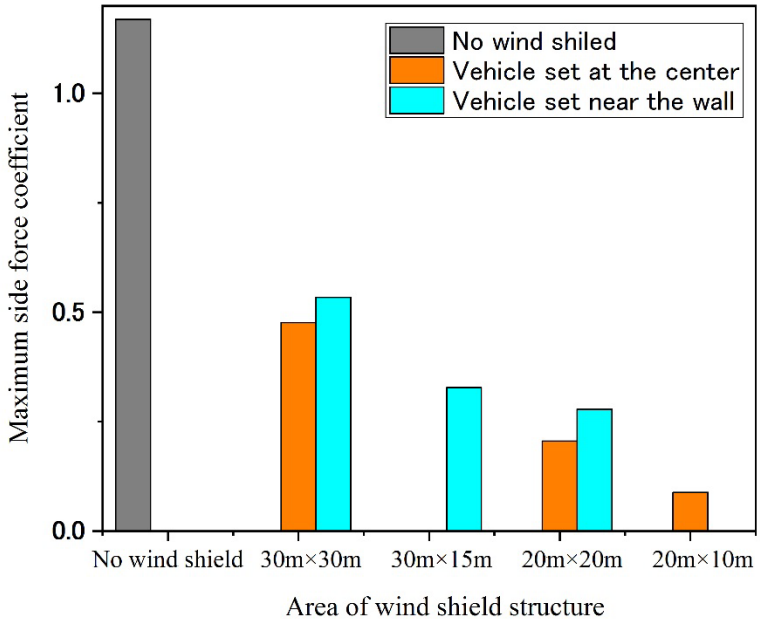

Figure 10. Maximum side force coefficient of each experimental cases.

DISCUSSION

Experimental results of Kopp et al. (2017) suggests that a fully loaded box truck can fail at 45-51m/s. Though the possibility of overturning failure depends on the truck geometry, weight distribution, wind pressure distribution and friction forces between the tyres and the ground, we simply try to evaluate the possibility of failure using the side force coefficients obtained above. If a vehicle is assumed to fail at 45 m/s, the corresponding side force, $F_{x,\,Fail}$, is calculated as follows.

$$F_{x,Fail} = \frac{45^2}{2}\rho HLC_{x,Case1} \tag{5}$$

On the other hand, the side force, $F_{x,Design}$, under a design wind condition is calculated as follows.

$$F_{x,Design} = \frac{100^2}{2}\rho HLC_{x} \tag{6}$$

In order for a vehicle to withstand the design wind condition, $F_{x,Design} < F_{x,\,Fail}$ is required, which leads to the following inequality condition.

$$\frac{C_x}{C_{x,Case1}} < \frac{45^2}{100^2} \approx 0.2 \tag{7}$$

The above requirement suggests that the 30m×30m wind shield structure is not good enough, and that the 20m×20m wind shield structure is around the critical condition. The 20m×10m wind shield structure will be able to protect a vehicle inside from its failure under the design wind condition or 100 m/s.

CONCLUSION

In this study, we have pursued for an effective wind shield structure to protect an emergence vehicle from tornado wind pressure. At first, the 2-D computational fluid dynamics method was employed to conduct a preliminary parametric survey to find out geometric parameters of importance in designing a wind shield structure. The 2-D computational results showed that the height of the wind shield structure relative to the vehicle height has a significant impact on the aerodynamic forces acting on the vehicle. It was also shown that the span distance has a significant impact on the drag force and lift force acting on the vehicle. That is, sufficient reduction effects of the drag and lift forces were confirmed for wind shield structures with the span distance within about 23.5m.

After the computational screening, wind tunnel tests were conducted to measure wind forces acting on a vehicle model with various span distances of wind shield structures. As the result of the wind tunnel experiment, the aerodynamic forces acting on the vehicle protected by the 30m-by-30m structure decreased by about 50%, while by 75% in the case of 20m-by-20m. A simplified estimation has suggested that the 30m×30m wind shield structure is not good enough, but that the 20m×10m wind shield structure will be able to protect a vehicle inside from its failure at wind speed of 100 m/s.

REFERENCES

Alonso-Estebanez, A., Del Coz Díaz, J.J., Alvarez Rabanal, F.P., Pascual-Munoz, P. (2017). "Performance analysis of wind fence models when used for truck protection under crosswind through numerical modeling," *Journal of Wind Engineering and Industrial Aerodynamics*, **168** 20–31

Bocciolone, M., Cheli, F., Corradi, R., Muggiasca, S., Tomasini, G. (2008). "Crosswind action on rail vehicles: wind tunnel experimental analyses," *Journal of Wind Engineering and Industrial Aerodynamics*, **96** 584–610.

Chen, N., Li, Y., Wang, B., Su, Y., Xiang, H. (2015). "Effects of wind barrier on the safety of vehicles driven on bridges," *Journal of Wind Engineering and Industrial Aerodynamics*, **143** 113-127.

Haan Jr., F.L., Sarkar, P.P., Kopp, G. A., Stedman, D. A. (2017). "Critical wind speeds for tornado-induced vehicle movements," *Journal of Wind Engineering and Industrial Aerodynamics*, **168** 1-8

Kopp, G. A., Hong, E., Gavanski, E., Stedman, D., Sills, D.M.L. (2017). "Assessment of wind speeds based on damage observations from the Angus (Ontario) Tornado of 17 June 2014," *Canadian Journal of Civil Engineering*, **44** 37-47.

Schmidlin T. et al., (2002). "Unsafe at any (Wind) Speed? Testing the Stability of Motor Vehicles in Severe Winds", *Bulletin of the American Meteorological Society*, **83** 1821-1830.

Xiang, H., Li, Y., Chen, S., Hou, G. (2018). "Wind loads of moving vehicle on bridge with solid wind barrier," *Engineering Structures*, **156** 188–196.